
The use of finite element analysis to model bone-implant contact with basal implants

Stefan Ihde, Dr.med.dent,^a Tomas Goldmann,^b Lucie Himmlova, MuDr.,^c and Zoran Aleksic, Dr,^d Gommiswald, Switzerland, Prague, Czech Republic, and Belgrade, Serbia
GOMMISWALD DENTAL CLINIC, CTU IN PRAGUE, INSTITUTE OF DENTAL RESEARCH, AND BELGRADE SCHOOL OF DENTISTRY

Objective. The purpose of this study was to develop a model that accurately represents the interface between bone and basal implants throughout the healing process.

Study Design. The model was applied to the biological scenario of changing load distribution in a basal implant system over time. We did this through finite element analysis (FEA, or finite element method [FEM]), using multiple models with changing bone-implant contact definitions, which reflected the dynamic nature of the interface throughout the bony healing process.

Results. In the simple models, peak von Mises stresses decreased as the bone-implant-contact definition was changed from extremely soft contact (i.e., immature bone during early loading) to hard contact (i.e., mature bone). In upgraded models, which more closely approximate the biological scenario with basal dental implant, peak von Mises stresses decreased at the implant interface; however, they increased at the bone interface as a harder contact definition was modeled. Further, we found a shift in peak stress location within the implants during different contact definitions (i.e., different stages of bony healing). In the case of hard contact, the peak stress occurs above the contact surface, whereas in soft contact, the stress peak occurs in the upper part of the contact area between bone and the vertical shaft of the implant. Only in the extreme soft contact definitions were the peak stresses found near the base plate of the implant.

Conclusion. Future FEM studies evaluating the functional role of dental implants should consider a similar model that takes into account bone tissue adaptations over time. (*Oral Surg Oral Med Oral Pathol Oral Radiol Endod* 2008;106:39-48)

Originally developed for solving structural problems in the aerospace industry, Finite Element Analysis/Method (FEA or FEM) has become a useful tool in the dental arena for predicting stress on implants and subsequent transfer of that stress to the surrounding bone, both key factors in overall implant success. Load transfer depends on type of loading, bone-implant interface, length and diameter of implants, shape and characteristics of the implant surface and prosthesis type, as well as the quality of the surrounding bone.¹ Poor load transfer may lead to complications such as implant

component fracture, abutment screw loosening, marginal bone loss, and loss of osseointegration.

Insertion of a basal implant requires a T-shaped slot cut into the alveolar bone, which will later be closed by bony healing with or without augmentation (Fig. 1). During early healing, the primary means of anchorage for the implant is through retention of the base plate in the basal, cortical jaw bone area, which in turn may be further secured by small screws to help fix the implant under immediate masticatory loads. The typical healing progression, which follows, is the transformation of a blood clot to fibrous tissue, which later mineralizes and becomes woven bone. This woven bone may provide additional stabilization to the implant, although it continues to be remodeled over time into an even more supportive secondary osteonal bone, the end result of the healing process (Fig. 2).

While the vertical aspect of a cylindrical implant must be placed in close contact to alveolar bone for primary stability, a basal implant, due to the nature of the insertion process, shows little or no contact in this area for some time. We have assumed that immediately after placement, only liquids or gels (e.g., blood clots) are present in the insertion slot, representing a situation with no contact or load transmission between bone and implant. Note that the blood clot or early fibrous tissues

This study was supported by grants from the Ministry of Education project No. MSM 6840770012 and by the Grant Agency of the Czech Republic under project No. 106/06/0849.

^aGommiswald Dental Clinic, Gommiswald, Switzerland.

^bDepartment of Mechanics, Biomechanics, and Mechatronics, Faculty of Mechanical Engineering, CTU in Prague, Prague, Czech Republic.

^cInstitute of Dental Research, Prague, Czech Republic.

^dAssociate Professor, Department of Periodontology, Belgrade School of Dentistry, Belgrade, Serbia.

Received for publication Mar 28, 2007; returned for revision Nov 22, 2007; accepted for publication Dec 6, 2007.

1079-2104/\$ - see front matter

© 2008 Mosby, Inc. All rights reserved.

doi:10.1016/j.tripleo.2007.12.005

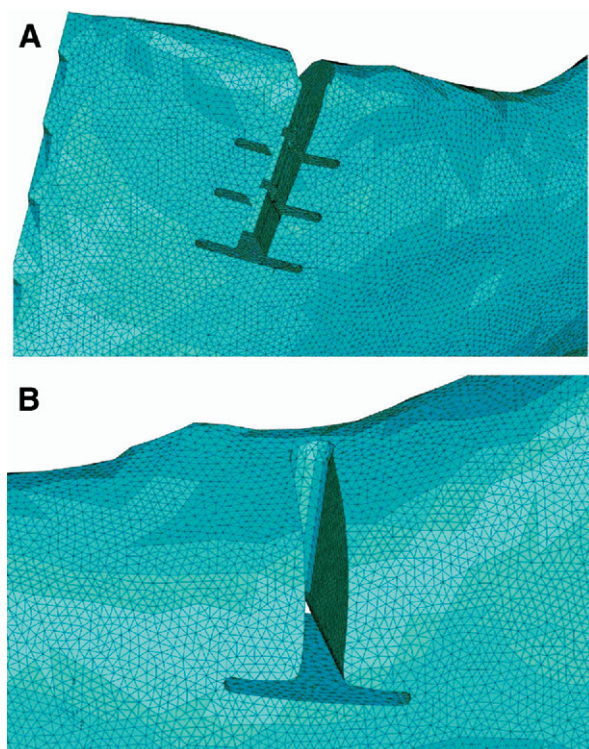


Fig. 1. **A**, T-shaped slot for a basal implant with 3 base plates in the anterior mandible. **B**, T-shaped slot for a basal implant with 1 base plate in the distal mandible

may transmit small forces, although with less effect on bone remodeling than with vertical implants. In the orthopedic literature, Geris et al.^{2,3} have modeled vertical implants in a “biphasic” or “poroelastic” tissue environment, which leads to an even distribution of stress throughout the peri-implant area. In their model, fluid velocity and maximum distortional strain are the primary stimuli behind differentiation.^{2,3}

Published histological findings from animal experiments⁴ using basal implants have shown that these implants will in fact osseointegrate over time even in those areas that have not had initial bone-to-implant contact, thus undergoing a secondary rather than a primary integration process in the alveolar area.⁴ This late integration has a continuing impact on load distribution within the implant and throughout the surrounding peri-implant tissue.

The purpose of this study was to develop a model that reflects the changes in bone structure and mineralization, as well as in the bone-implant contact, and to calculate the subsequent changes in stresses on the implants and bone resulting from mastication. We have attempted to address the changing intraosseous load distribution along the vertical aspect of a basal implant

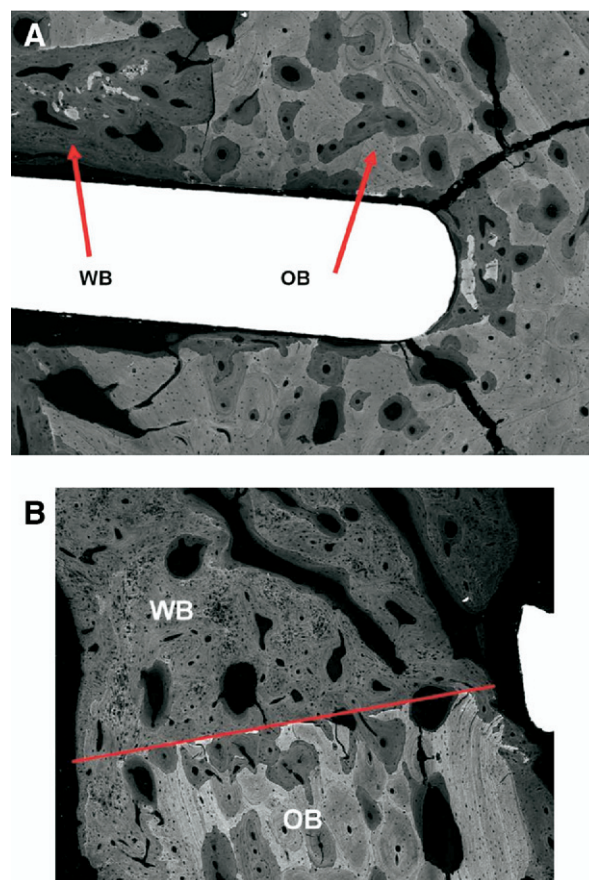


Fig. 2. Radial cross-cut through the vertical slot area of a single base plate basal implant (histological x-ray view, actual picture size 4.5×4.5 mm; 3.5 months postop, dog mandible). **A**, In areas without space between the inserted implant and the bone only osteonal remodeling is found. Larger spaces are partially filled with woven bone. **B**, Area above the red line shows vertical slot insertion path filled with woven bone that is just beginning to remodel. The area below the red line shows remodeled osteonal bone where the remodeling process is more advanced than in the upper woven bone area. WB, woven bone; OB, osteonal bone.

by using a range of contact definitions in FEM modeling.

MATERIAL AND METHODS

Models were created with ABAQUS 6.6-5 (Abaqus Inc., Providence, RI).⁵ Selected contacts between bone and implant were SOFT and HARD. The HARD contact relationship minimizes the penetration of slave nodes into the master surface and does not allow the transfer of tensile stress across the interface. The SOFT contact relationship allows the penetration of the slave nodes into the master surface. Penetration-contact/pressure relationships are defined in sections below and in

Table I. Model parameters and results

Model no.	BIC definition	Quantitative inputs	Equivalent von Mises stress at peak (MPa)	Peak stress location	Figure no.
1	Extremely soft	Hole diameter: 3 mm Vertical Load: 114.6 N Horizontal Load: 23.4 N Vestibulo Oral: 17.1 N Fixation: Bottom part of shaft and bone	190.9	Near base plate	4
2	Soft	Hole diameter: 3 mm Vertical Load: 114.6 N Horizontal Load: 23.4 N Vestibulo Oral: 17.1 N Fixation: Bottom part of shaft and bone	118	Below and above upper contact definition area edge	5
3	Hard	Hole diameter: 3 mm Vertical Load: 114.6 N Horizontal Load: 23.4 N Vestibulo Oral: 17.1 N Fixation: Bottom part of shaft and bone	109.9	Above upper contact definition area edge	6
4	Extremely Soft Upgraded	Fixation: Cut above mandibular ramus Vertical Load: 114.6 N Horizontal Load: 23.4 N Vestibulo Oral: 17.1 N	Implant: 645 Bone: 32	Near base plate	7
5	Soft Upgraded	Fixation: Cut above mandibular ramus Vertical Load: 114.6 N Horizontal Load: 23.4 N Vestibulo Oral: 17.1 N	Implant: 624 Bone: 47	Below the bone edge	8
6	Hard Upgraded	Fixation: Cut above mandibular ramus Vertical Load: 114.6 N Horizontal Load: 23.4 N Vestibulo Oral: 17.1 N	Implant: 536 Bone: 211	Above the bone edge	9

Table I. The implant and the abutment were considered to have “tied” contact (i.e., completely connected, with stresses being transmitted unchanged in quantity and direction). In all following models (basic cubical and upgraded models) we assumed that typical masticatory forces would be 114.6 N in the vertical, 17.1 N in the vestibular/oral, and 23.4 N in the horizontal direction (i.e., between implants).⁶ For basic cubical models, the vestibular/oral direction corresponds (Figs. 3 to 6) to axis “1,” the horizontal component corresponds to axis “2,” and vertical direction corresponds to axis “3.” Directions of loading were chosen with reference to anatomical disposition of mandible model in a case of upgraded models.

The HARD and SOFT contacts were tested on a simple model of a bone-cube with the inserted shaft of the basal implant (Fig. 3). Bone and implant were assumed to be linear and elastic (isotropic). Young’s modulus/Poisson ratio for bone and implant were 14,000 MPa/0.34 and 100,000 MPa/0.34, respectively.

Fig. 3 shows the bone and implant model, with the upper part of the shaft loaded and the bone and implant fixed at the base only. The model was meshed by “C3D8R” ABAQUS elements.⁵ The data input defining contact between shaft and bone can be found in Table I. This situation is identical to the inserted basal implant with healed bone. In addition, there is a vertical slot on the insertion side.

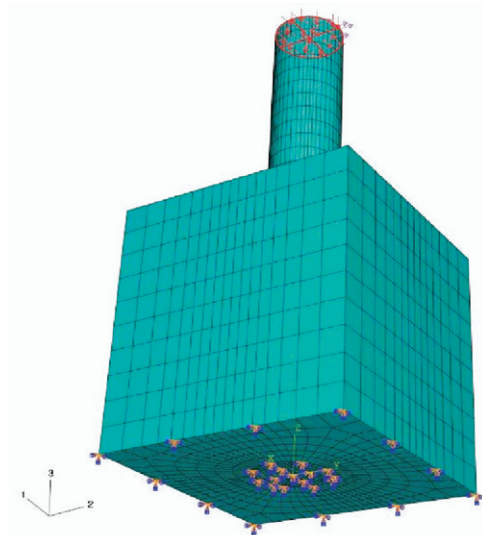


Fig. 3. Finite element model of the implant shaft inside the bone created for testing different contact definitions: Loading area (red); fixation of shaft and bone is shown by markers at the base of the cube.

We created 6 models, which represent the healing continuum from baseline through full implant osseointegration, as described below. See Table I for model parameters and results.

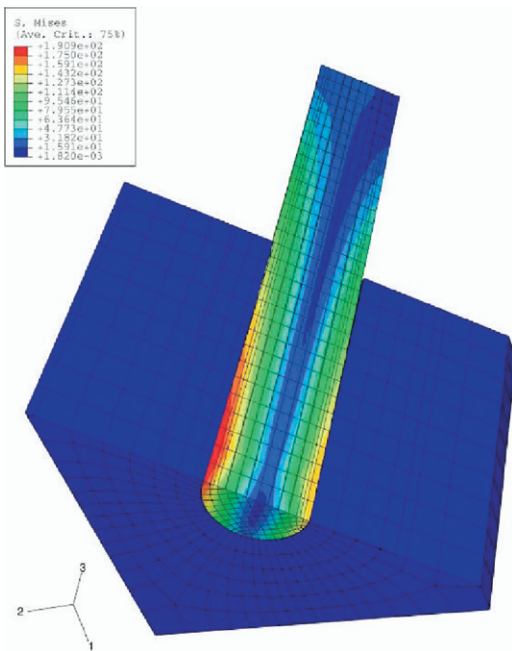


Fig. 4. Distribution of von Mises stresses for the extremely SOFT contact definition in a simplified model.

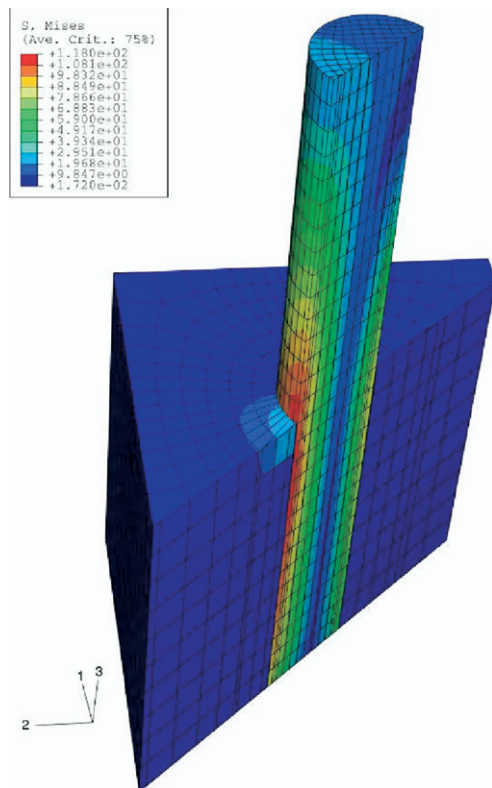


Fig. 5. Distribution of von Mises stresses for the SOFT contact definition in a simplified model.

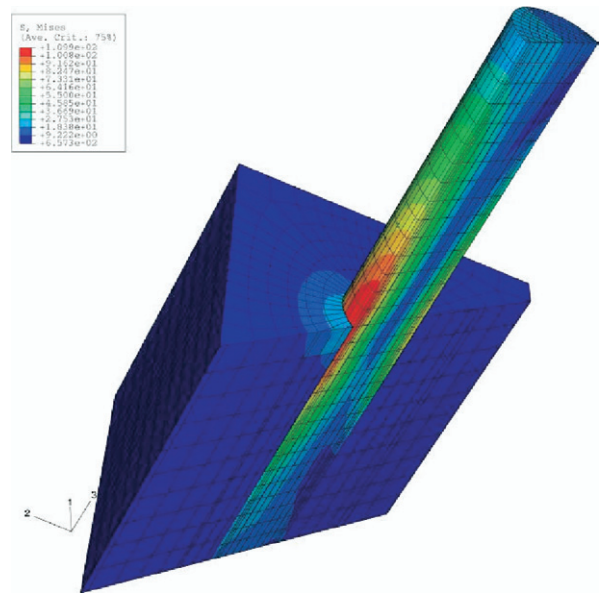


Fig. 6. Distribution of von Mises stresses for the HARD contact definition in a simplified model.

The difference between models 1, 2, and 3 lies in the definition of the contact behavior. When using the ABAQUS program, the contact behavior of 2 surfaces (one of them being defined in ABAQUS as a MASTER SURFACE, the second as a SLAVE SURFACE) is formulated through the pressure-overclosure relationship. The term pressure in this context represents contact pressure between 2 deformable bodies.

At each slave node that can come into contact with a master surface we construct a measure of overclosure (penetration of the node into the master surface) and calculate the relative slip. These kinematic measures are then used to introduce surface interaction theories for contact and friction.

The default contact pressure-overclosure relationship used by ABAQUS is referred to as the HARD contact model. It assumes that the surfaces transmit no contact pressure unless the nodes of the slave surface contact the master surface. There is no limit to the magnitude of contact pressure that can be transmitted when the surfaces are in contact. The HARD contact relationship minimizes the penetration of slave nodes into the master surface and does not allow the transfer of tensile stress across the interface. This corresponds to our Model 3, which represents HARD contact. In this case, contact description in ABAQUS syntax is defined as follows.

*Surface Interaction, name=HARD

1.,

*Surface Behavior, pressure-overclosure=HARD

Models 1 and 2 represent in the ABAQUS software the so-called SOFT or SOFTENED contact relationship. This definition allows significant penetration (overclosure) of SLAVE surface nodes into MASTER surface. Three types of SOFTENED contact relationships are available in ABAQUS. The pressure-overclosure relationship can be prescribed by using a linear law, a tabular piecewise-linear law, or an exponential law. The SOFTENED contact pressure-overclosure relationships might be used to model a soft, thin layer on one or both surfaces. The tabular option was used for creating models 1 and 2 as follows.

Model 1: Extremely SOFT

*Surface Interaction, name=extreme soft

1.,

*Surface Behavior, pressure-overclosure=TABULAR

0., 0.

6, 0.6

12., 1.2

Model 2: SOFT

*Surface Interaction, name=_Int-1-Property

1.,

*Surface Behavior, pressure-overclosure=TABULAR

0., 0.

0.01, 0.02

230., 0.05

where the first column of tabular definition represents value of pressure and the second column represents overclosure. The symbol “*” represents the beginning of the ABAQUS command.

Model 1: Extremely SOFT contact

This model was designed to represent early bone reconstruction. Hence, we assumed that the bone directly surrounding the endosseous parts of the implant was much softer than the implant body, based on histological observations of basal implants. The exact degree of mineralization cannot be quantified.

Model 2: SOFT contact

This model was designed to represent advanced stage of bone reconstruction. After a considerable healing time, the degree of mineralization in peri-implant bone increases for 2 reasons: (1) immediately, woven bone fills the voids around the implants and demonstrates fast but not structured mineralization,⁷ and (2) osteonal bone is remodeled simultaneously with the primary mineralization taking place after approximately 180 days.⁸ Even unmineralized, remodeled osteonal bones

may provide a considerable resistance for the implant. Although only a few tags of old bone provide the holding scaffold, the refilled osteons, equipped with high osmotic pressure, may act as a supporting cushion, which fills the voids.

Model 3: HARD contact

This model was designed to represent a fully osseointegrated implant with a high degree of mineralization in the bone surrounding the implant. After more than 12 months, full remineralization of bone can be expected. At this time, bone gives maximum resistance against the implants.

Models 4, 5, and 6: Upgraded

The models were upgraded to more realistic conditions for basal implants in bone to validate our previous simple contact definition and to give a broader basis to evaluate the effect of implant deformation and the stress distribution on the bony healing process. We used a nonhomogeneous, linear elastic isotropic material definition. Nonhomogeneous material properties were obtained from the gray scale values of a computed tomography (CT) scan of a human mandible, using the areas of the second molar for the single base plate implant, and the area of the canine for the triple base plate implant. The gray scale values were transformed to a 100 linear elastic material model (Young modulus and Poisson Ratio). The gray scale was calibrated, using point 14 (Xi-point), as described by Schwartz-Dabney and Dechow⁹ (Fig. 1) in 2003. This model allowed us to distinguish between cortical and spongy bone. The models were examined under the 3 scenarios described above (i.e., extremely SOFT contact, SOFT contact, and HARD contact) representing increased bone maturity with each subsequent model.

RESULTS

Models, contact descriptions, quantitative inputs, maximum equivalent von Mises stress (MPa), and stress peak locations are presented in Table I. For the associated figures, the abutment has been removed.

In the simple models (Models 1 to 3), the peak stress shifted as the bone-implant-contact definition was changed from extremely SOFT to HARD (Figs. 4 to 6). The highest equivalent von Mises stresses (190.9 MPa) were seen at the peak of the extremely SOFT model and were located near the base plate (Fig. 4). Peak stress continued to decline in the SOFT and HARD models (118 and 109.9 MPa, respectively). The peak stress was located below and above the upper contact definition area in the SOFT model; however, it was located above the upper contact definition area in the HARD model.

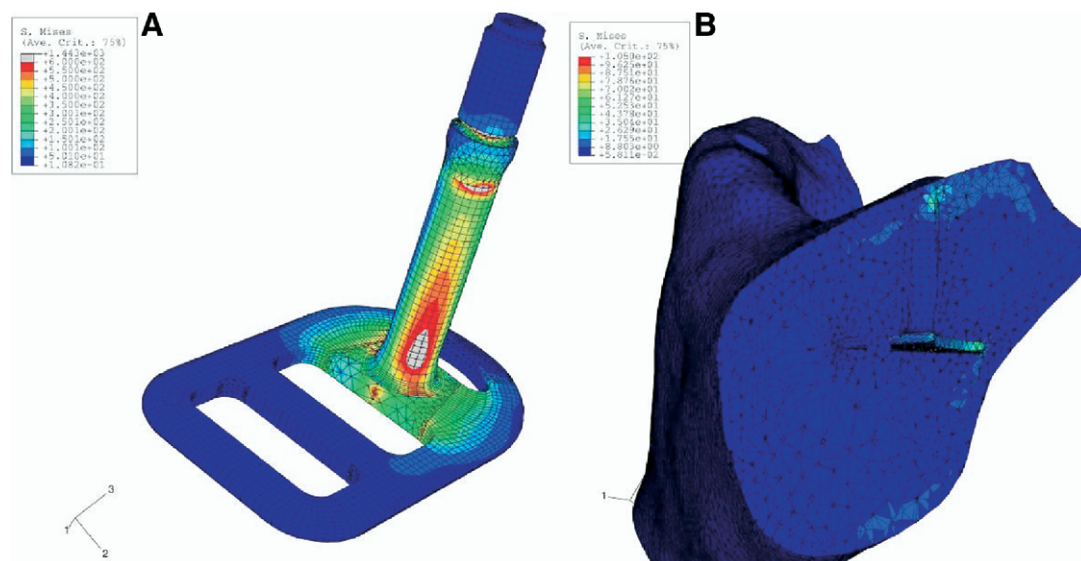


Fig. 7. Distribution of von Mises stresses for extremely SOFT contact definition in an upgraded model of a real basal implant. **A**, Stress distribution within the implant. **B**, stress distribution within the bone.

In the upgraded models (Models 4 to 6), peak von Mises stress decreased at the implant interface; however, they increased at the bone interface as a harder contact definition was modeled (i.e., more mature bone). Peak von Mises stress for implants was 645, 624, and 536 MPa for the extremely SOFT, SOFT, and HARD contact definitions, respectively. Peak stresses for bone were 32, 47, and 211 MPa for extremely SOFT, SOFT, and HARD contacts, respectively. Furthermore, peak stress location shifted from the base plate (extremely SOFT) to below the bone edge and then above the bone edge (SOFT and HARD) (Figs. 7 to 9).

DISCUSSION

The purpose of this study was to develop a model that reflects changes in bone structure and mineralization and the bone-implant contact situation, and then to calculate the subsequent changes in stresses imposed by mastication onto the system. We found that in the simple models (Models 1 to 3), the peak von Mises stresses decreased as the bone-implant-contact definition was changed from extremely SOFT to HARD. In the upgraded models, which more closely approximate the biological scenario with basal implants (Models 4 to 6), peak von Mises stresses decreased at the implant interface; however, they increased at the bone interface as a harder contact definition was modeled (i.e., more mature bone). Further, we found a shift in stress peak location within the implants during different contact definitions (i.e., different stages of bony healing). In the

case of hard contact (i.e., mature bone), the stress peak occurs above the contact surface, whereas in soft contact (i.e., immature bone during early loading) the stress peak occurs in the upper part of the contact area between bone and the vertical shaft of the implant. Only in the extreme SOFT contact definitions are the peak stresses found near the base plate of the implant. These results, which are displayed in Table I and Figs. 4 to 9, are shown only for implants with 1 base plate. They are, however, similar to the results obtained when using implants with 3 base plates (Fig. 10).

When we further examined the location of peak stresses (Fig. 9, A), we discovered peak stress “2” below the upper shoulder is caused by the notch at the vertical implant part. It is present in all calculations. Peak stress “1” stems from the design of the implant and is also permanent. However, peak stress “3” changes location depending on the progress of integration. It is found near peak stress “1” in the hard contact situation (i.e., in the fully integrated implant).

All presented models were loaded by 1 uniform etalon loading, which is, according to our knowledge, most liable for the real physiological loading during mastication in order to keep clarity of the article; the main objective of this text is the presentation of a novel access to model the bone-implant interface with respect to the healing process of basal implants. However, all our models can be easily extended to evaluate the influence of different loading situations and different loads. This could be an interesting direction of future research.

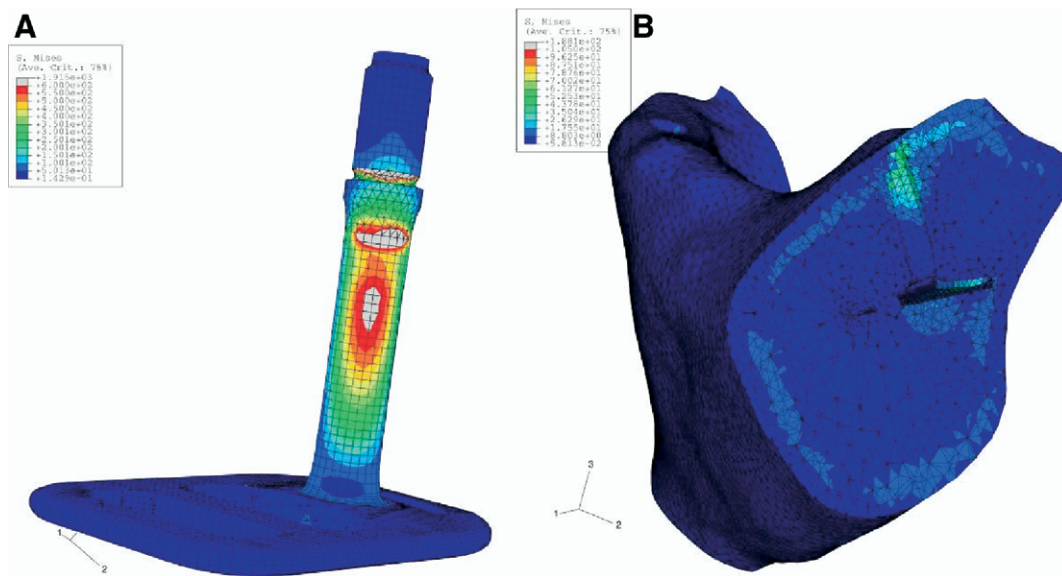


Fig. 8. Distribution of von Mises stresses for typical SOFT contact definition in an upgraded model of a real basal implant. **A**, Stress distribution within the implant. **B**, stress distribution within the bone.

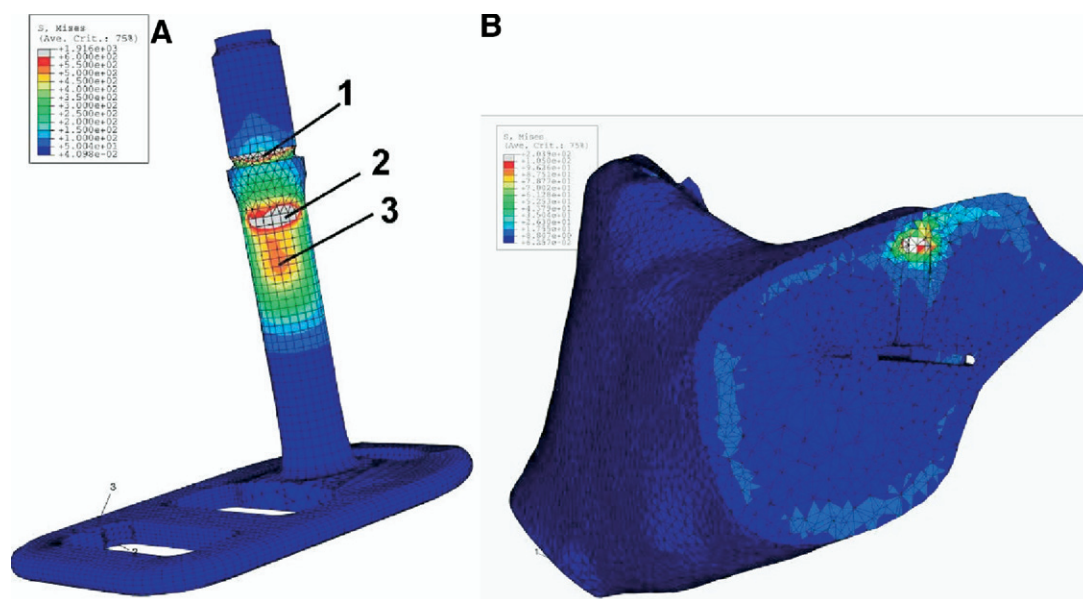


Fig. 9. Distribution of von Mises stresses for HARD contact definition in an upgraded model of a real basal implant. **A**, Stress distribution within the implant. **B**, stress distribution within the bone.

We do not know if or how our findings can be applied to conventional screw implants. Since crestal implants lack the retention offered by the base plate used in basal implants, bone-implant contact must be tight, with primary stability of utmost importance. This differs from our model; in which no contact is present in the vertical implant part at baseline.

These findings, however, do apply to basal implant design and other similar prosthetic systems. Maximum stresses on basal implants are expected to occur not only in the area of the penetration into the bone, but also, depending on the mineralization of the bony interface and the degree of osseointegration, in the vertical piece well below the bony crest. The same expect-

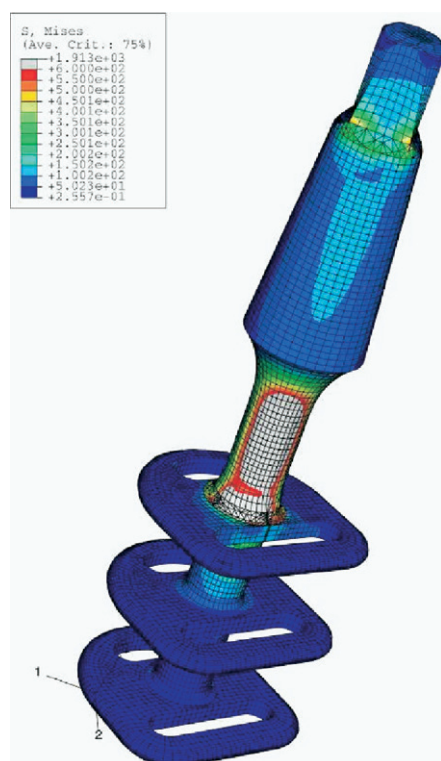


Fig. 10. An example of distribution of von Mises stresses for an implant with 3 base plates.

tation may be applied to basal implants, which have been placed trans-sinusly without augmentation. Those implants will not integrate around the vertical piece at all and hence lateral stresses will always occur near the base plate.

There is a fairly large body of literature examining FEM in dental implantology. Before performing our study, we conducted a literature search with the purpose of reviewing recently published studies (2000 to present) evaluating FEM in dental implant or orthopedic implant systems seeking to find studies that may have reported on modeling relevant to basal implant systems. MEDLINE was searched to identify studies reporting data on FINITE ELEMENT METHOD in dental and orthopedic implants. We discovered that few dental implant studies appeared to take into account the dynamic nature of the bony healing process in relation to the contact definitions of the FEM model. This was not surprising since most studies report on crestal implantology in which the implant is placed in cortical bone at baseline, which represents a more static environment. However, healing after basal implant placement is analogous to fracture healing and, as such, the bony healing process must be considered and modeled accordingly.



Fig. 11. A picture of a typical 1-piece basal implant with 1 asymmetrical base plate and a fixed head for cementation.

We did identify a select number of papers in the dental implant literature that emphasized the importance of a dynamic model. Brand et al.¹⁰ propose the incorporation of 2 types of modelling: hierarchical and iterative. In the case of hierarchical modeling, tissues are modeled in multiple layers, from micro- to macroscopic,^{10,11} allowing the investigator to more realistically study the local environment of interest. Iterative modeling addresses the idea that the environment around an implant does not remain the same for long (i.e., it recognizes the ongoing healing process and the changing stress patterns that accompany these changes). Our models and scenarios presented here show the usefulness of the iterative model in fracture healing.

In the orthopedic implant literature, 2 studies were identified that used the finite element method to predict tissue adaptation. Geris et al.³ numerically modeled the process of peri-implant tissue differentiation inside a bone chamber that was placed in a rabbit tibia. Two dimensional (2D) and 3D models were created of the tissue inside the chamber. A number of loading conditions, corresponding to those applied in the rabbit experiments, were simulated. Under loads of 50- μ m amplitude, granulation tissue differentiated into bone in a large volume of the bone chamber. At the interface

between tissue and implant, cartilage was favored. At the bottom of the chamber, high strain and fluid velocity restricted differentiation beyond fibrous tissue. Both the predicted tissue phenotypes and the tissue ingrowth into the chamber showed a qualitative agreement with the results of the rabbit experiments. (Differentiation at 160- μ m amplitude was not yet experimentally determined.) Because of the limited number of animal experiments (4) and the observed interanimal differences, no quantitative comparisons were made. However, the authors felt that the results supported the feasibility of the implemented theory to predict the mechano-regulation of the differentiation process inside the bone chamber. In another study, Geris et al.² acknowledge the trend toward immediate or early loading in orthopedic implants, and investigated the way in which loading (model parameters) may affect normal, early tissue healing and differentiation pathways. They used a bone chamber to create a mechanically isolated *in vivo* environment in which the influence of different parameters on the tissue response around loaded implants could be investigated, and then created 2D finite element models of the tissue inside the bone chamber. In a biphasic model, under 50- μ m amplitude, the entire chamber was filled with bone except for a small layer of cartilage (250 μ m) around the implant. For the 160- μ m displacement, bone formed only in the chamber perforations. In a linear elastic model, after 1 loading cycle, results were similar to the biphasic model. However, additional cycles yielded quite different results. Under the elastic model, tissue deformation is localized to the tissue-implant interface. However, with the biphasic model, the deformation effect is spread over the entire chamber, changing the calculated strain values. The authors noted that fluid flow has a clear contribution to bone maturation. Increased programming capacity and modeling sophistication are bringing FEM closer toward the ideal of a customized treatment plan for the individual, especially in orthopedics. Our study is an attempt to accomplish this by modeling different contacts simulating the changes in implant and bone behavior over time.

It is important to assess peak stresses at the bone and implant interface in dental implants in an attempt to simulate real biological conditions. A functional stress range of 200 to 700 psi¹² (or 1.4 to 5.0 MPa¹) has been reported as necessary to maintain existing alveolar bone height in dental implant systems. Less stress may lead to bone atrophy, and more may lead to pathologic bone remodeling and resorption.^{1,12} Our computations in cortical and cancellous are above 5 MPa (i.e., the functional stress range); therefore, in the range of bone remodeling. Following injury, bone tends to become softer not only at the point of injury but also over a

larger surrounding area due to the broad remodeling process. Full remineralization is not achieved until 1 to 2 years postinjury.¹³ This phenomenon is due to retarded and long-lasting phase remodeling and the delay in mineralization of the new osteons.⁸ Additionally, during the early phases of remodeling following basal implant placement, no direct contact between bone and implant is present. Rather, contact develops over time, either through osteonal remodeling of newly formed woven bone or through direct bridging of secondary osteons over the osteotomy slots. A stabilized implant in a bone area, which is under heavy remodeling, may appear less stiffly integrated than an implant that has been integrated for years. This does not directly relate to the usability of the implant, as long as the masticatory forces applied are below the threshold. However, crack accumulation would irreversibly destroy those areas of the bony interface, which guarantee fixation of the implant inside the bone.

The lack of direct bone-implant contact at the vertical part of basal implants means that no direct stimulation can be expected during early healing. The fibrous tissue developing from the blood clot may transmit some pressure, but no contact or stimulation from the implant under loading conditions in the crestal area. Hence the bony healing follows the regular pathways of repair and is unaffected by the implant until, at a later stage of healing and integration, the crestal areas are captured by the bone and start being stimulated or influenced. After healing, peak stresses are located in the crestal bone areas (Figs. 6 and 9).

Basal implants are known to show no crater-like bone defects, possibly due to the polished vertical implant surface area.¹⁴ Our results suggest that a strong functional stimulation of the crestal bone area just underneath the penetration region may also be a contributing factor. Occasional fractures of overloaded basal implants have been observed clinically. Only fractures of the horizontal struts of the base plates or slightly above the base plates have been found in the first approximately 48 months (Fig. 7). Late fractures (occurring during a HARD contact situation) tend to occur somewhere in the upper area of the implant.

In the case of basal implants, masticatory forces are transmitted by the basal plate, which is locked in cortical bone (i.e., there is no contribution of the vertical piece necessary to achieve primary stability). The ingrowth of the osteonal bone from the walls of the osteotomy follows *after* woven bone has been formed to fill the voids. The question of whether micromovements of the shaft (vertical or horizontal) enhance bony growth or maturity still remains to be answered.

CONCLUSION

This study has demonstrated that a model can be developed that closely simulates the biological changes in bone from immediate implant placement until full osseointegration at a high degree of mineralization is achieved. This is particularly important in dental implantology as bony tissue adapts over time and should be modeled accordingly. In our upgraded models, which closely approximate the biological scenario of basal implants, we found peak von Mises stresses decreased at the implant interface; however, they increased at the bone interface as a harder contact definition was modeled (i.e., more mature bone). Further, we were able to identify specifically where the peak stresses occurred on the implant during these different phases of bone healing. Future FEM studies evaluating the functional role of dental implants should consider a similar model that takes into account bone tissue adaptations over time.

REFERENCES

1. Geng JP, Tan KB, Liu GR. Application of finite element analysis in implant dentistry: a review of the literature. *J Prosthet Dent* 2001;85:585-98.
2. Geris L, Van Oosterwyck H, Vander Sloten J, Duyck J, Naert I. Assessment of mechanobiological models for the numerical simulation of tissue differentiation around immediately loaded implants. *Comput Methods Biomech Biomed Engin* 2003;6:277-88.
3. Geris L, Andreykiv A, Van Oosterwyck H, Sloten JV, van Keulen F, Duyck J, et al. Numerical simulation of tissue differentiation around loaded titanium implants in a bone chamber. *J Biomech* 2004;37:763-9.
4. Ihde S, Principles of BOI. Heidelberg: Springer; 2005.
5. Abaqus Manual. Available at: www.abaqus.com.
6. Merisce-Stern R, Assal P, Buerger W. Simultaneous force measurements in 3 dimensions on oral endosseous implants in vitro and in vivo: a methodological study. *Clin Oral Implants Res* 1996;7:378-86.
7. Rüedi TP, Buckley RE, Moran CG, editors. *AO principles of fracture management*. 2nd ed. Stuttgart: AO Publishing, Thieme; 2000.
8. Martin RB, Burr DB, Sharkey NA. *Skeletal tissue mechanics*. New York: Springer; 1998.
9. Schwartz-Dabney CD, Dechow PC. Variations in cortical material properties throughout the human dentate mandible. *Am J Phys Anthropol* 2003;120:252-77.
10. Brand RA, Stanford CM, Swan CC. How do tissues respond and adapt to stresses around a prosthesis? A primer on finite element stress analysis for orthopaedic surgeons. *Iowa Orthop J* 2003;23:13-22.
11. Be'ery-Lipperman M, Gefen A. A method of quantification of stress shielding in the proximal femur using hierarchical computational modeling. *Comput Methods Biomech Biomed Engin* 2006;9:35-44.
12. DeTolla DH, Andreana S, Patra A, Buhite R, Comella B. Role of the finite element model in dental implants. *J Oral Implantol* 2000;26:77-81.
13. Atkinson PJ, Powell K, Woodhead C. Cortical structure of the pig mandible after the insertion of metallic implants into alveolar bone. *Arch Oral Biol* 1977;22:383-91.
14. Ihde S, Konstantinovic VS. Comparison and definition of pathological peri-implant symptoms and possible therapeutic measures with basal and crestal implants. *Dent Implantol Update* 2005;9:122-33.

Reprint requests:

Stefan Ihde, MuDr
Gommiswald Dental Clinic
Dorfplatz 11
8737 Gommiswald/SG
Switzerland
dr.ihde@bluewin.ch
dr.ihde@implant.com